Available online at www.sciencedirect.com
SCIENCE DIRECT®
Journal of Sound and Vibration 262 (2003) 509–527
JOURNAL OF SOUND AND VIBRATION
www.elsevier.com/locate/jsvi

Acoustic attenuation of hybrid silencers

A. Selamet[a,b,*], I.J. Lee[a,b], N.T. Huff[c]

[a] *Department of Mechanical Engineering, The Ohio State University, Columbus, OH 43210-1107, USA*
[b] *The Center for Automotive Research, The Ohio State University, Columbus, OH 43212-1443, USA*
[c] *Owens Corning Automotive, Novi, MI 48377, USA*

Received 13 March 2002; accepted 26 October 2002

Abstract

The acoustic attenuation of a single-pass, perforated concentric silencer filled with continuous strand fibers is investigated first theoretically and experimentally. The study is then extended to a specific type of hybrid silencer that consists of two single-pass perforated filling chambers combined with a Helmholtz resonator. One-dimensional analytical and three-dimensional boundary element methods (BEM) are employed for the predictions of the acoustic attenuation in the absence of mean flow. To account for the wave propagation in absorbing fiber, the complex-valued characteristic impedance and wave number are measured. The perforation impedance facing the fiber is also presented in terms of complex-valued characteristic impedance and wave number. The effects of outer chamber diameter and the fiber density are examined. Comparisons of predictions with the experiments illustrate the need for multi-dimensional analysis at higher frequencies, while the one-dimensional treatment provides a reasonable accuracy at lower frequencies, as expected. The study also shows a significant improvement in the acoustic attenuation of the silencer due to fiber absorption. Multi-dimensional BEM predictions of a hybrid silencer demonstrate that a reactive component such as a Helmholtz resonator can improve transmission loss at low frequencies and a higher duct porosity may be effective at higher frequencies.

1. Introduction

The recent improvements in the fibrous material properties combined with their broadband acoustic dissipation characteristics make such materials potentially desirable for implementation in silencers. The sound absorption characteristics of such materials are well established in the

*Corresponding author. Department of Mechanical Engineering, The Ohio State University, 206 West 18th Ave., Columbus, OH 43210-1107, USA. Tel.: +1-614-292-4143; fax: +1-614-292-3163.
E-mail address: selamet.1@osu.edu (A. Selamet).

0022-460X/03/$ - see front matter © 2003 Elsevier Science Ltd. All rights reserved.
doi:10.1016/S0022-460X(03)00109-3

literature [1]. The use of fibers may prove particularly effective when their dissipative characteristics are combined with the reactive silencers, leading to hybrid configurations.

The acoustic behavior of an expansion chamber lined (locally reacting) with absorbing material has been investigated by Craggs [2] using the finite element method. He has shown that (1) the absorbing material increases the magnitude and changes the shape of transmission loss, and (2) increasing the thickness of absorbing material reduces the number of domes and shifts the peak frequencies of transmission loss. Peat and Pathi [3] have used finite element method to examine the effects of induced non-uniform steady flow within absorbing material. However, neither Ref. [2] nor Ref. [3] considers the perforated duct. Wang [4] has analyzed a single-pass perforated absorbing silencer in terms of a one-dimensional decoupled method. To account for the acoustic characteristics of absorbing material, Wang uses complex-valued characteristic impedance and wave number, which depend on tortuosity, Prandtl number, and porosity. While simulation results have been presented for a variety of parameters, such results have not been validated by experimental work. Empirical expressions of Sullivan and Crocker [5], originally developed for perforations in the absence of absorbing material, have been used for the perforation impedance. Thus, the effect of absorbing material on the perforation impedance has been neglected in Wang's work. Recently, Kirby [6] has investigated circular concentric dissipative silencers with mean flow in terms of an analytical closed-form solution by using a series expansion of Bessel and Neumann functions to solve governing equations and mode matching technique at the interfaces where the cross-sectional areas change. However, his predictions overestimate the effect of perforation impedance due to the neglect of the interactions among perforations.

The material properties are essential in studying the behavior of absorbing silencers. Delany and Bazley [7] have suggested empirical expressions for the characteristic impedance and wave number for fibrous absorbing material as a function of frequency and flow resistance. They have found that the flow resistance is determined by fiber size and bulk density. Recently, Song and Bolton [8] have estimated the characteristic impedance and wave number of porous material by using measured pressures and a transfer matrix. The elements of the transfer matrix are evaluated from a single microphone approach and then the reciprocity of the matrix is used to calculate the acoustic properties of absorbing material. The characteristic impedance and wave number estimated by the transfer matrix method agree with the empirical expressions of Delany and Bazley [7]. Their conclusion that the acoustic property of the material is independent of the sample depth and termination condition is also adopted in the present study.

Absorbing materials are typically used in combination with perforated ducts or screens, resulting in an interaction between them. Acoustic characteristics of the porous layer facing perforations have been investigated by Ingard and Bolt [9], who have considered the perforation as an addition of mass. Recently, Kirby and Cummings [10] have extended this work by investigating two types of perforations, circular and louvered plates, with and without porous backing. They have concluded that (1) the porous material increases the perforation impedance, and (2) the reactance term facing absorbing material has both real and imaginary components, with imaginary part of the reactance resulting in an increase in resistance of the total perforation impedance. They have suggested that single hole data may be applicable for multi-hole perforations, thereby neglecting the interactions between the holes.

Selamet et al. [11] have developed the analytical and BEM for single-pass concentric perforated dissipative silencers with fixed outer chamber diameter (164.4 mm) and two duct porosities (2%

and 8%). The comparison of predictions with experimental results shows the significant effect of absorbing material on the perforation impedance and consequently on the overall acoustic performance of dissipative silencers. The present study extends this earlier work to examine the effect of outer chamber diameter for single-chamber dissipative silencers and the acoustic characteristics of a hybrid silencer that consists of two dissipative chambers combined with a reactive component between them. The three-dimensional BEM code developed originally for single-pass perforated silencers [11] have been modified to apply to two-dimensional axisymmetric hybrid or multi-chamber silencers in the present work. The objectives of the present study are then to (1) investigate theoretically and experimentally the acoustic performance of uniformly perforated absorbing silencers with different outer chamber diameter and material density; and (2) examine acoustic behavior of a hybrid silencer that is a combination of dissipative and reactive components. The present analytical and computational study assumes that (1) the absorbing material is homogeneous, isotropic, and rigid frame; (2) there is no mean flow; (3) the thickness of the perforated duct is much smaller than the wavelength; (4) the characteristic impedance and wave number are independent of the depth of porous material; and (5) the temperature is uniform throughout silencer. Complex-valued empirical expressions are used for the acoustic properties of perforation impedance and absorbing material. The transmission loss predictions from the one-dimensional decoupled approach and the multi-dimensional BEM are compared to experimental results obtained from an extended impedance tube set-up.

2. Theory

The theory associated with the sound propagation and attenuation is described next in terms of a single-pass, concentric absorbing silencer depicted in Fig. 1 with d_1 and d_2 being the diameters of uniformly perforated inner duct and solid outer chamber, respectively, and ℓ the length of silencer. This section includes the one-dimensional decoupled method, multi-dimensional BEM, and the acoustic impedance of perforates, as well as the complex-valued characteristic impedance and the wave number of absorbing material.

2.1. One-dimensional decoupled method

Assuming harmonic planar wave propagation in both the center perforated duct and expansion chamber (Fig. 1), the continuity and momentum equations yield, in the absence of

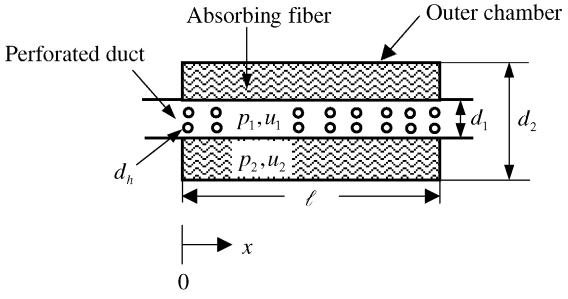

Fig. 1. A single-pass perforated absorbing silencer.

mean flow [4],

$$\frac{\mathrm{d}^2 p_1}{\mathrm{d}x^2} + \alpha_1 p_1 + \alpha_2 p_2 = 0, \tag{1}$$

$$\frac{\mathrm{d}^2 p_2}{\mathrm{d}x^2} + \alpha_3 p_1 + \alpha_4 p_2 = 0, \tag{2}$$

where

$$\alpha_1 = k^2 - \frac{4}{d_1}\frac{\mathrm{i}k}{\tilde{\zeta}_p}, \quad \alpha_2 = \frac{4}{d_1}\frac{\mathrm{i}k}{\tilde{\zeta}_p}, \tag{3,4}$$

$$\alpha_3 = \frac{4d_1}{d_2^2 - d_1^2}\frac{\tilde{\rho}}{\rho_0}\frac{\mathrm{i}k}{\tilde{\zeta}_p}, \quad \alpha_4 = \tilde{k}^2 - \frac{4d_1}{d_2^2 - d_1^2}\frac{\tilde{\rho}}{\rho_0}\frac{\mathrm{i}k}{\tilde{\zeta}_p}, \tag{5,6}$$

and ρ_0 and k denote, respectively, the density and the wave number in air, and $\tilde{\rho}$ and $\tilde{k}$ the complex-valued dynamic density and the wave number in the absorbing material, and $\tilde{\zeta}_p$ the non-dimensionalized acoustic impedance of perforation. Eqs. (1)–(6) may be combined to yield [11]

$$\begin{bmatrix} p_1(0) \\ Z_0 u_1(0) \end{bmatrix} = \begin{bmatrix} T_{11} & T_{12} \\ T_{21} & T_{22} \end{bmatrix} \begin{bmatrix} p_1(\ell) \\ Z_0 u_1(\ell) \end{bmatrix}, \tag{7}$$

which defines the transfer matrix elements, T_{ij}; $Z_0 = \rho_0 c_0$ being the characteristic impedance of air and c_0 the speed of sound. Assuming a duct with constant cross-sectional area, the transmission loss can then be calculated from the transfer matrix as

$$TL = 20 \log_{10}\left(\tfrac{1}{2}|T_{11} + T_{12} + T_{21} + T_{22}|\right). \tag{8}$$

2.2. Three-dimensional boundary element method

The wave propagation is governed by the Helmholtz equation in the perforated duct (domain 1),

$$\nabla^2 p_1 + k_1^2 p_1 = 0, \tag{9}$$

and in the outer chamber (domain 2),

$$\nabla^2 p_2 + \tilde{k}_2^2 p_2 = 0, \tag{10}$$

where k_1 and $\tilde{k}_2$ are wave numbers in air and absorbing material, respectively. Applying Green's theorem to Helmholtz equation results in a boundary integral equation [12,13]

$$C_i(\alpha_i) p_i(\alpha_i) = \int_{\Gamma_i} \left[G_i(\alpha_i, \beta_i) \frac{\partial p_i(\beta_i)}{\partial \vec{n}} - p_i(\beta_i) \frac{\partial G_i(\alpha_i, \beta_i)}{\partial \vec{n}} \right] \mathrm{d}\Gamma_i(\beta_i), \quad i = 1, 2, \tag{11}$$

where α_i and β_i are points on the boundary surface Γ_i, $C_i(\alpha_i)$ is a coefficient, and $G_i(\alpha_i, \beta_i)$ is the Green's function or fundamental solution given by, for domain 1,

$$G_1(\alpha_1, \beta_1) = \frac{\mathrm{e}^{-\mathrm{j}k_1|\alpha_1 - \beta_1|}}{4\pi|\alpha_1 - \beta_1|}, \tag{12}$$

and for domain 2,

$$G_2(\alpha_2, \beta_2) = \frac{e^{-j\tilde{k}_2|\alpha_2-\beta_2|}}{4\pi|\alpha_2 - \beta_2|}. \tag{13}$$

Integrating Eqs. (11) and discretizing the boundary surfaces into a number of elements and then applying rigid boundary condition on the solid wall yields [12,13]

$$\begin{Bmatrix} \{p_1^i\} \\ \{p_1^o\} \\ \{p_1^p\} \end{Bmatrix} = \begin{bmatrix} [TA_{11}] & [TA_{12}] & [TA_{13}] \\ [TA_{21}] & [TA_{22}] & [TA_{23}] \\ [TA_{31}] & [TA_{32}] & [TA_{33}] \end{bmatrix} \begin{Bmatrix} \{u_1^i\} \\ \{u_1^o\} \\ \{u_1^p\} \end{Bmatrix}, \tag{14}$$

$$\{p_2^p\} = [TB]\{u_2^p\}, \tag{15}$$

where u_1 and u_2 are normal outward acoustic velocities at the boundaries of the perforated duct and outer chamber, respectively, and superscripts i, o and p denote inlet, outlet, and perforate. The impedance matrices of outer chamber ($[TA]$) and inner duct ($[TB]$) may be coupled by the boundary conditions at the perforate interface. The acoustic velocity continuity at the interface yields

$$\{u_1^p\} = -\{u_2^p\}, \tag{16}$$

where the negative sign is assigned since u_1 and u_2 are normal outward acoustic velocities for each domain. Assuming a perforation thickness much smaller than the wavelength, pressure difference at the perforate may be expressed as

$$\{p_1^p\} - \{p_2^p\} = Z_0\tilde{\zeta}_p\{u_1^p\}, \tag{17}$$

where $\tilde{\zeta}_p$ is the non-dimensionalized perforate acoustic impedance. Combining Eqs. (14)–(17) yields the impedance matrix $[TI]$ of a single-chamber, defined by [12,13]

$$\begin{Bmatrix} \{p_1^i\} \\ \{p_1^o\} \end{Bmatrix} = \begin{bmatrix} TI_{11} & TI_{12} \\ TI_{21} & TI_{22} \end{bmatrix} \begin{Bmatrix} \{u_1^i\} \\ \{u_1^o\} \end{Bmatrix}, \tag{18}$$

where

$$[TI_{11}] = [TA_{11}] + [TA_{13}](\zeta[I] - ([TA_{33}] + [TB]))^{-1}[TA_{31}], \tag{19a}$$

$$[TI_{12}] = [TA_{12}] + [TA_{13}](\zeta[I] - ([TA_{33}] + [TB]))^{-1}[TA_{32}], \tag{19b}$$

$$[TI_{21}] = [TA_{21}] + [TA_{23}](\zeta[I] - ([TA_{33}] + [TB]))^{-1}[TA_{31}], \tag{19c}$$

and

$$[TI_{22}] = [TA_{22}] + [TA_{23}](\zeta[I] - ([TA_{33}] + [TB]))^{-1}[TA_{32}]. \tag{19d}$$

For a single-chamber silencer, the average of acoustic pressure and velocity from Eq. (18) at nodes on the inlet and outlet planes determine first the transfer matrix of Eq. (7), followed by the transmission loss through Eq. (8). For multiple-chambers, the overall impedance matrix of the silencer is obtained by connecting the impedance matrix of each chamber in terms of continuity of acoustic pressure and velocity [12,13]. The overall impedance matrix then yields the transfer matrix and therefore the transmission loss of the silencer in view of Eq. (8).

2.3. Acoustic impedance of perforates

In Eqs. (3)–(6) and (17), the perforate impedance $\tilde{\zeta}_p$ relates the acoustic pressures in the inner duct and the outer chamber through the interface. Sullivan and Crocker [5] presented empirical expressions for perforate acoustic impedance considering hole interactions. For low velocities through the holes, the acoustic impedance is given by

$$\tilde{\zeta}_p = [0.006 + \mathrm{i}k(t_w + 0.75d_h)]/\phi, \tag{20}$$

where t_w is the duct wall thickness, d_h the perforate hole diameter, ϕ the porosity. However, Eq. (20) has been developed in the absence of filling material. For perforations facing absorbing material, such an equation needs to be modified in view of the work by Kirby and Cummings [10] as

$$\tilde{\zeta}_p = \left[0.006 + \mathrm{i}k\left\{t_w + 0.375d_h\left(1 + \frac{\tilde{Z}_a}{Z_0}\frac{\tilde{k}}{k}\right)\right\}\right]/\phi. \tag{21}$$

It is assumed that the interactions among perforates through absorbing material are the same as those through air. In comparison with Eq. (20), the use of complex values for the characteristic impedance $\tilde{Z}_a$ and wave number $\tilde{k}$ in Eq. (21) changes both real and imaginary parts of the perforation impedance. When the medium is air, $\tilde{Z}_a/Z_0$ and $\tilde{k}/k$ become unity, thereby reducing Eq. (21) to Eq. (20). Thus, Eqs. (20) and (21) have been employed in this study for silencers without and with filling material, respectively. Significantly different predictions resulting from Eqs. (20) and (21) have been demonstrated in Ref. [11].

2.4. Wave propagation in absorbing material

The absorption of acoustic waves in filling material is mainly due to viscous dissipation, which may be expressed in terms of complex-valued characteristic impedance and wave number [14]. The imaginary part of the wave number accounts for the decay of the waves, which is called the attenuation constant. Due to complex structure of the absorbing material, the acoustic properties are often determined experimentally. Delany and Bazley [7] presented empirical expressions for the complex-valued characteristic impedance and wave number of an absorbing material which are included in Appendix A.

The present study uses texturized fiber glass roving. The texturization process separates 4000 filament roving strands of fiber glass into individual filaments by turbulent air flow (Silentex process [15]). The average diameter of the individual filaments in the roving strand is 24 μm with the distribution shown in Fig. 2. The degree to which the strands are separated into individual filaments affects both the complex-valued wave number and the impedance of the absorbing material. The physical and chemical properties of various absorptive materials and their relative durability in simulated automotive silencer operations are described by Huff [15]. The acoustic properties of the absorbing material used in the present study have been measured using the two cavity method and fitted by Nice [16]:

$$\frac{\tilde{Z}_a}{Z_0} = [1 + 0.0855(f/R)^{-0.754}] + \mathrm{i}[-0.0765(f/R)^{-0.732}], \tag{22}$$

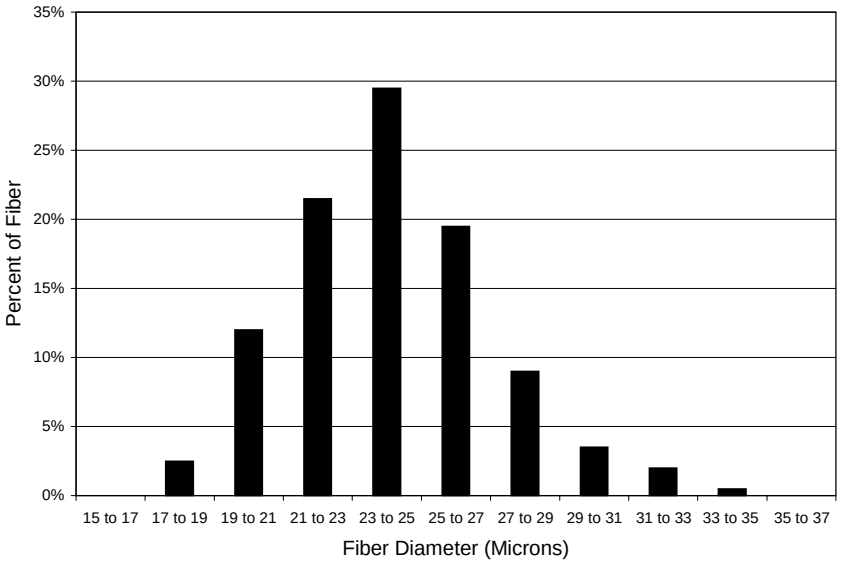

Fig. 2. Fiber diameter distribution chart.

$$\frac{\tilde{k}}{k} = [1 + 0.1472(f/R)^{-0.577}] + \mathrm{i}[-0.1734(f/R)^{-0.595}] \tag{23}$$

for $\rho_0 = 1.1555\,\mathrm{kg/m^3}$, where f (Hz) is frequency and R (mks Rayls/m) the flow resistivity. $\tilde{Z}_a$ and $\tilde{k}$ from Eqs. (22) and (23), and R are critical in predicting the acoustic behavior of dissipative silencers since they characterize the dissipative wave propagation through fiber material. For the measurement technique as well as the acoustic characteristics of some other absorbing materials, including fiberglass board, shoddy, and cellulose, the reader is referred to Nice and Godfrey [17]. Similar to Eqs. (A.1) and (A.2) of Delany and Bazley [7], Eqs. (22) and (23) depend on the flow resistivity and frequency. The measured flow resistivity R in Eqs. (22) and (23) are 4896 and 17378 Rayls/m for 100 and 200 g/l material densities, respectively [16]. Figs. 3 and 4 show the real and imaginary parts of characteristic impedance and wave numbers measured by Delany and Bazley [7] and Nice [16]. For both complex-valued numbers the imaginary parts are essentially identical and the real parts show some deviation while exhibiting qualitatively similar trends.

3. Results and discussion

An impedance tube test set-up is used in this study to obtain transmission loss of silencers applying the two-microphone technique. Wideband white random noise or a single frequency sine wave can be generated by a loudspeaker. For silencers that have high transmission loss including hybrid and long dissipative silencers, the single frequency sine wave is used selectively to create sufficient power transmitted to the downstream of the silencer. The speed of sound during

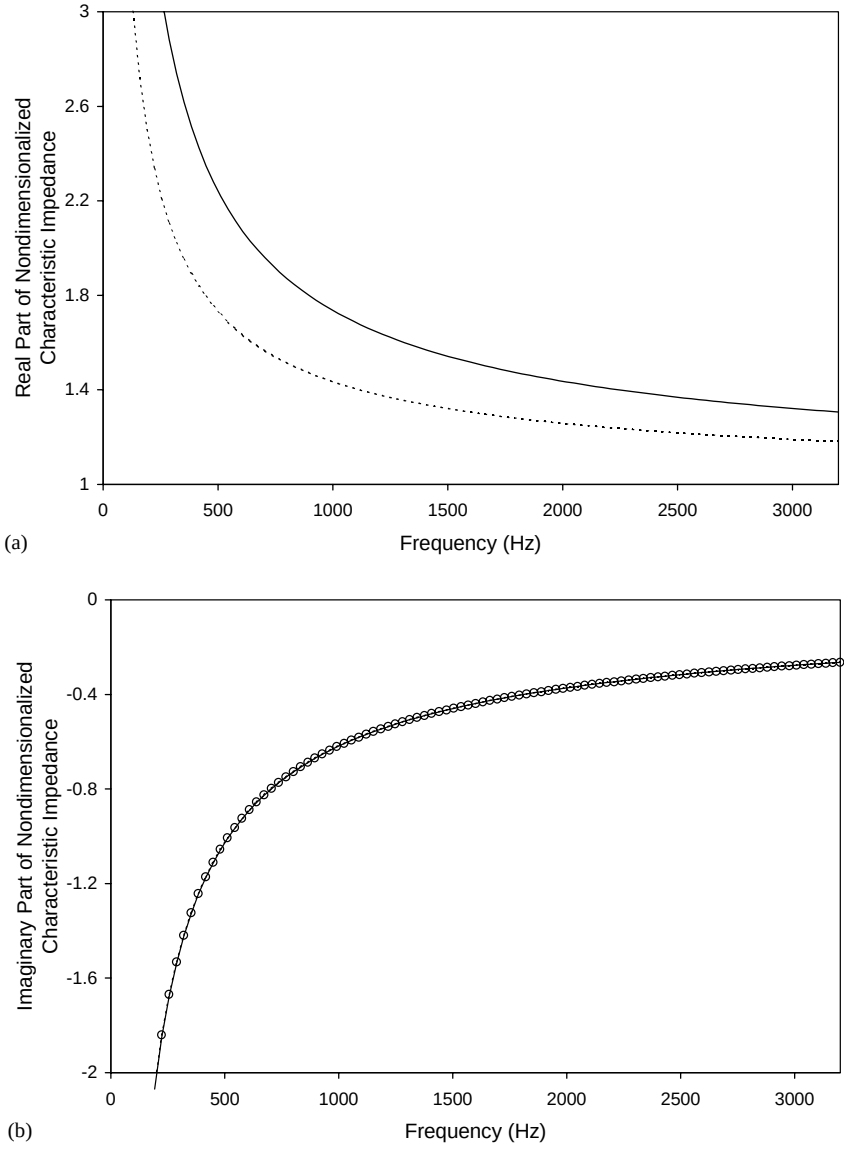

Fig. 3. Comparison of non-dimensionalized characteristic impedance of absorbing materials with $\rho_f = 200$ g/l: (a) real part:----, Delany and Bazley [7]; ——, Nice [16]: (b) imaginary part: o, Delany and Bazley [7]; ——, Nice [16].

acoustic experiments is 343.1 m/s, which is also adopted in predictions. For further details of the experimental set-up, refer to Ref. [18].

The present study considers: (1) two single-pass concentric silencers of length $\ell = 257.2$ mm, uniformly perforated ducts of diameter $d_1 = 49.0$ mm, perforate hole diameter $d_h = 2.49$ mm, wall thickness of perforated ducts $t_w = 0.9$ mm, a porosity of 8%, and outer chamber diameters of $d_2 = 101.0$ and 164.4 mm; (2) a single-pass silencer of the first part with outer chamber diameter of 164.4 mm now combined with a reactive silencer, thereby leading to a hybrid design. The results

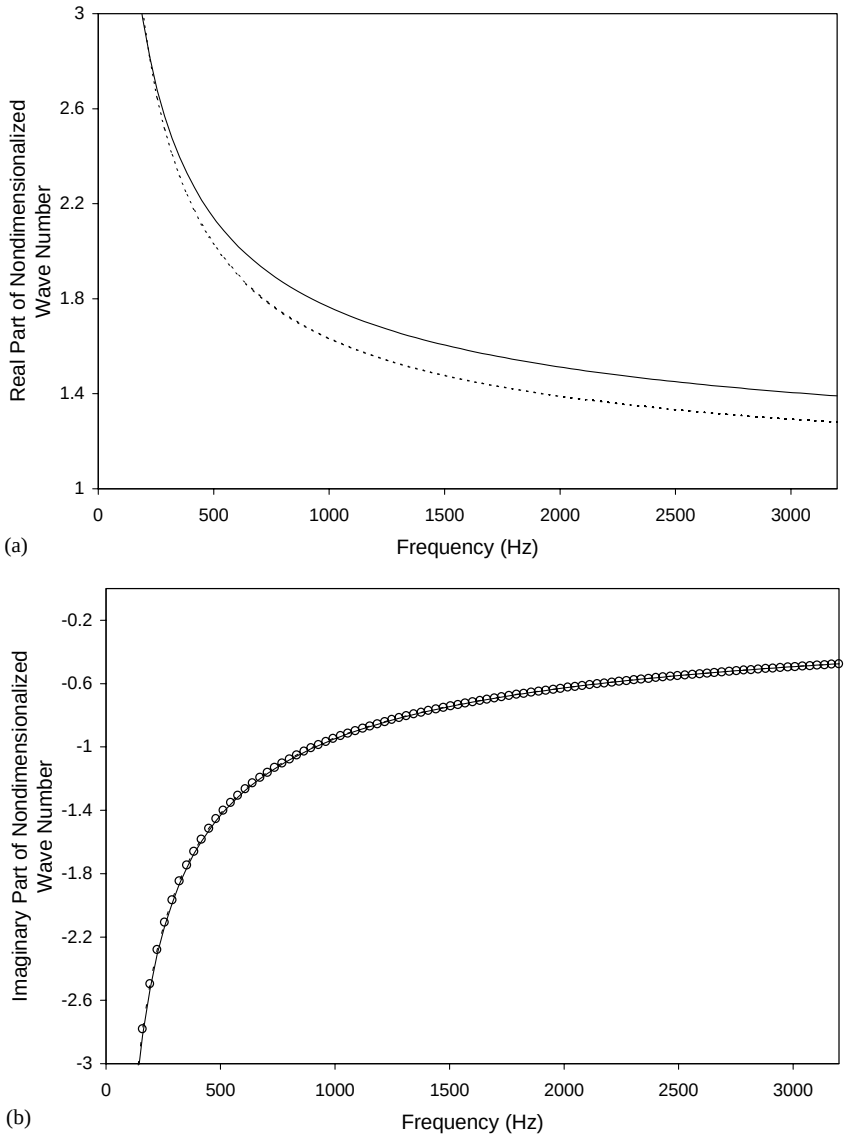

Fig. 4. Comparison of non-dimensionalized wave number of absorbing materials with $\rho_f = 200$ g/l: (a) real part:----, Delany and Bazley [7]; ——, Nice [16]: (b) imaginary part: o, Delany and Bazley [7]; ——, Nice [16].

of these configurations are described next, while the impact of two different duct porosities (2% and 8%) with a fixed outer chamber diameter (164.4 mm) has already been discussed elsewhere [11].

3.1. *Single-pass perforated filled silencer*

Fig. 5 shows the measured transmission loss for the empty versus filled (with $\rho_f = 100$ and 200 g/l absorbing material) perforated silencers with $d_2 = 164.4$ mm. Both silencers with absorbing

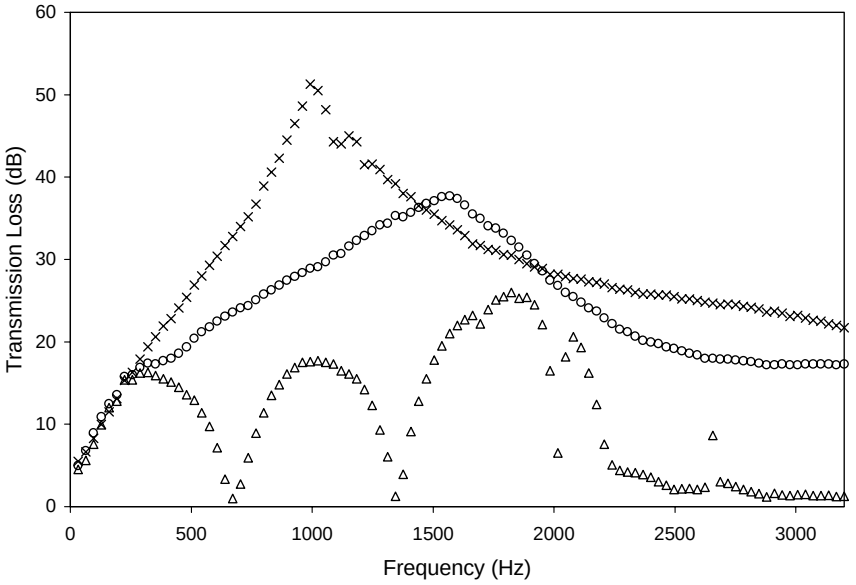

Fig. 5. Experimental results; transmission loss of single-pass perforated absorbing silencer with $d_2 = 164.4$ mm: Δ, without filling material; o, $\rho_f = 100$ g/l; ×, $\rho_f = 200$ g/l.

material have significantly higher acoustic attenuation than the one with no filling above 280 Hz. The silencer with no filling has several broadband attenuation domes up to 2000 Hz, resembling the behavior of expansion chambers. The addition of absorbing material changes the acoustic behavior of the silencer drastically, by transforming the repeating domes to a single broad peak. Increasing the density of the absorbing material from $\rho_f = 100$ to 200 g/l increases the peak transmission loss, as well as shifting its location to a lower frequency. Note that at frequencies below 280 Hz, the filling material has no influence on the transmission loss of purely reactive system.

For an empty silencer with $d_2 = 164.4$ mm, the one-dimensional analytical and the multi-dimensional BEM are compared with the experiments in Fig. 6. While the BEM shows a good agreement with experiments for the overall frequency range except around 2100 Hz, the one-dimensional predictions start to deviate from measurements at 1500 Hz and fails completely at higher frequencies. The inaccuracy of one-dimensional analysis above 1500 Hz is due to the neglect of non-planar wave propagation. Both the one-dimensional analytical and the BEM employ Eq. (21) [5] for the perforation impedance.

The predictions for two silencers with $d_2 = 164.4$ mm and filling densities $\rho_f = 100$ and 200 g/l are compared with experiments in Figs. 7 and 8, respectively. While the BEM predictions show a reasonable agreement with experiments in the entire frequency range of interest, the one-dimensional analysis approach appears to capture the trends until the peaks around 1500 and 800 Hz in Figs. 7 and 8, respectively, and deviate significantly above these values. Thus, the one-dimensional method starts failing at lower frequencies with increasing filling density. For the predictions presented in Figs. 7 and 8, it is important to note that Eq. (21) is used to account for the effect of absorbing material on the perforation impedance.

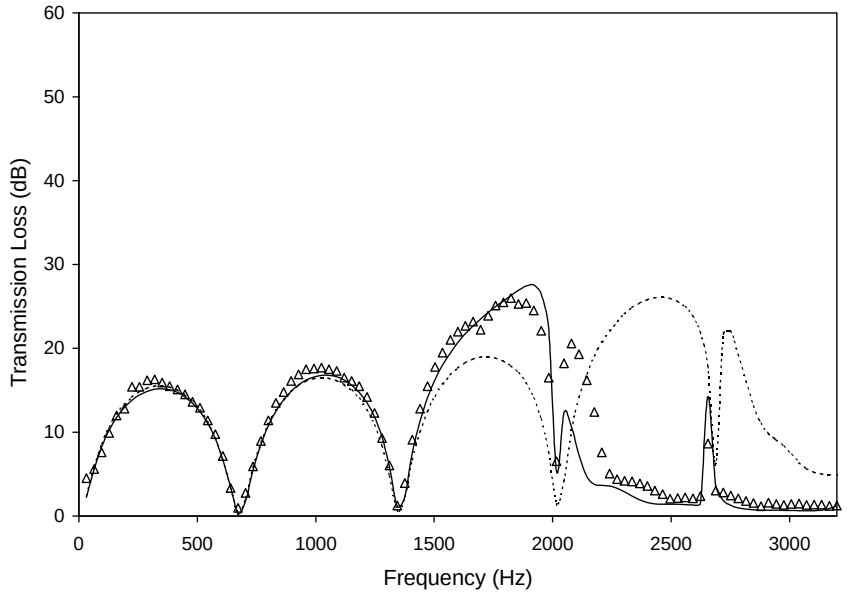

Fig. 6. Transmission loss of single-pass perforated absorbing silencer with $d_2 = 164.4$ mm and no filling material: Δ, experiment; ----, 1-D analytical; ——, BEM.

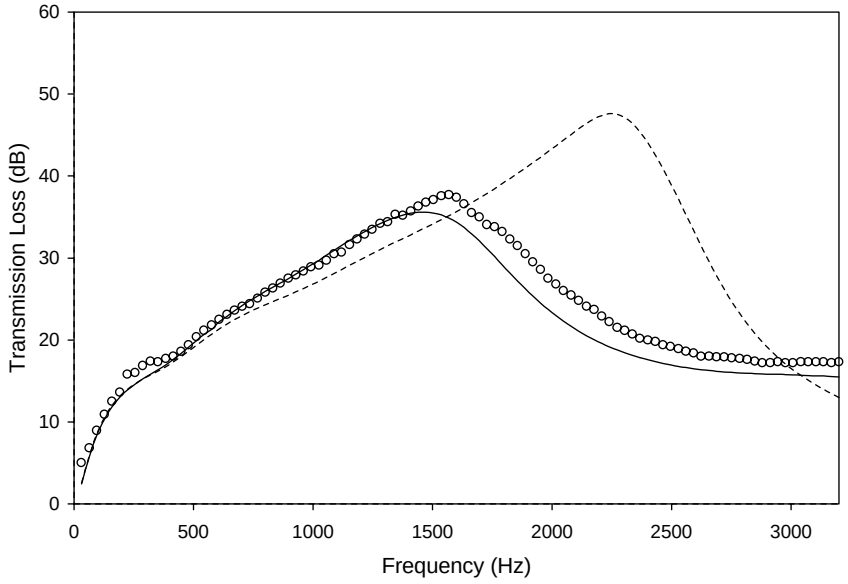

Fig. 7. Transmission loss of single-pass perforated absorbing silencer with $d_2 = 164.4$ mm and $\rho_f = 100$ g/l: o, experiment; ----, 1-D analytical; ——, BEM.

Fig. 9 shows the effect of the outer chamber diameter ($d_2 = 101.0$ and 164.4 mm) on the transmission loss for single-chamber silencers with ($\rho_f = 100$ and 200 g/l) and without absorbing material. For the reactive silencers, the frequencies of the maximum and minimum transmission

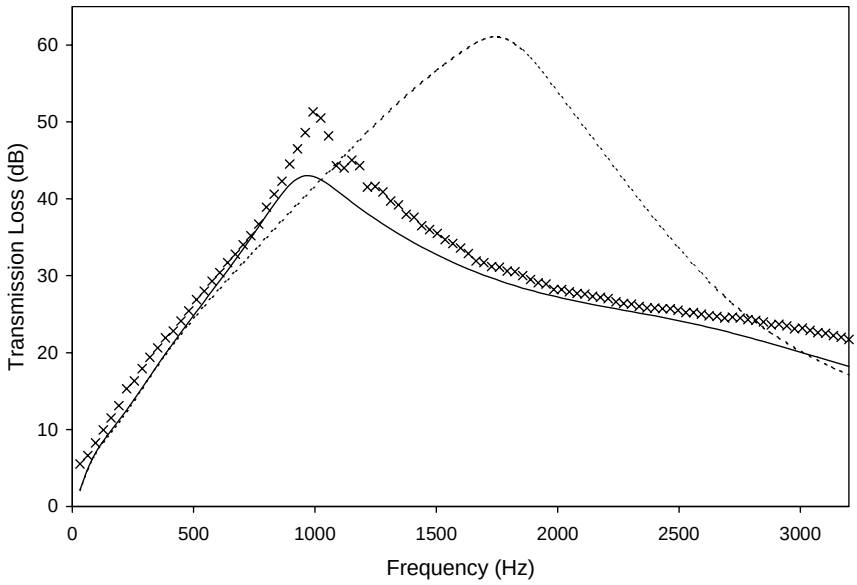

Fig. 8. Transmission loss of single-pass perforated absorbing silencer with $d_2 = 164.4$ mm and $\rho_f = 200$ g/l: $\times$, experiment; - - - -, 1-D analytical; ——, BEM.

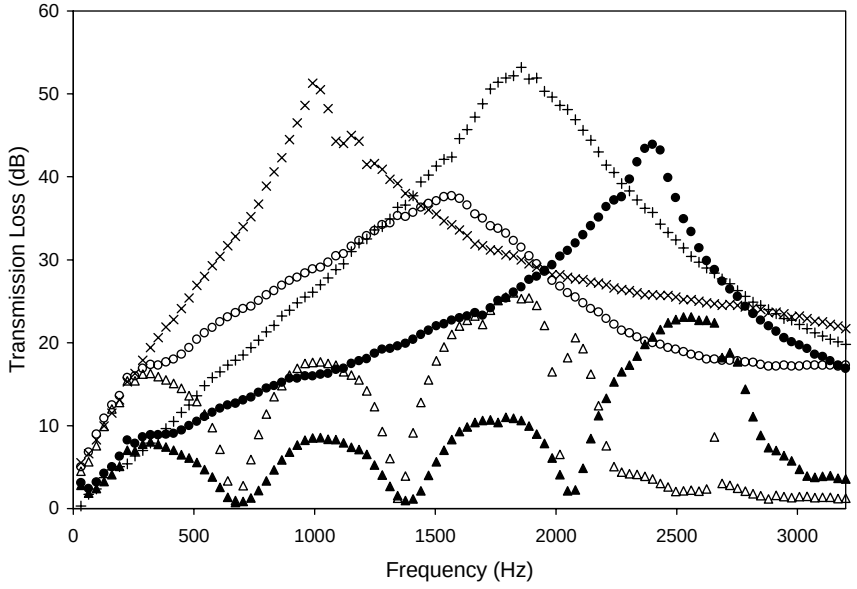

Fig. 9. Experimental results: transmission loss of single-pass perforated absorbing silencer: Δ, $d_2 = 164.4$ mm and without filling material; o, $d_2 = 164.4$ mm and $\rho_f = 100$ g/l; $\times$, $d_2 = 164.4$ mm and $\rho_f = 200$ g/l; ▲, $d_2 = 101.0$ mm and without filling material; ●, $d_2 = 101.0$ mm and $\rho_f = 100$ g/l; +, $d_2 = 101.0$ mm and $\rho_f = 200$ g/l.

loss are the same until about 2 kHz which is near the cut-off frequency of larger diameter chamber, and with the larger chamber exhibiting in general higher transmission losses, as expected. The overall shape of transmission loss for a reactive silencer is determined by the length

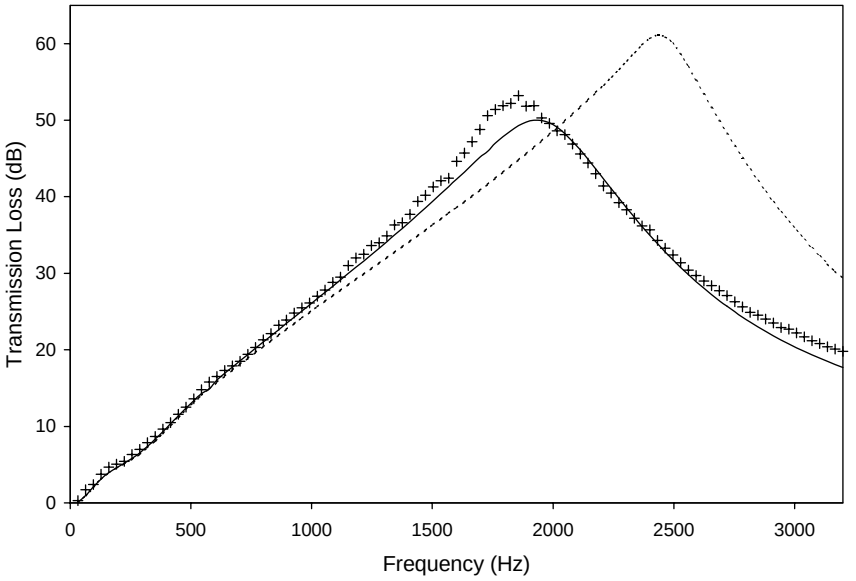

Fig. 10. Transmission loss of single-pass perforated absorbing silencer with $d_2 = 101.0$ mm and $\rho_f = 200$ g/l; +, experiment; - - - -, 1-D analytical; ——, BEM.

and diameter of the outer chamber with rest of the geometry fixed. For dissipative silencers, higher filling density lowers the resonance frequency and increases the magnitude of transmission loss for both silencers. Increase in chamber diameter from 101.0 to 164.4 mm shifts the resonance to lower frequencies for both material densities. Unlike the reactive chambers, the larger diameter chamber does not necessarily exhibit a higher transmission peak.

Fig. 10 compares the predictions and experiments for a dissipative silencer with $d_2 = 101.0$ mm and $\rho_f = 200$ g/l. Similar to the silencer with $d_2 = 164.4$ mm, the BEM shows a good agreement with experiments for the overall frequency range, while the one-dimensional predictions start to deviate from measurements at higher frequencies due to propagation of the first radial mode.

3.2. Hybrid silencer

As shown in Figs. 5 and 9, absorbing material is effective only at relatively higher frequencies. The resonators can be used to enhance the acoustic performance of these silencers at low frequencies. Thus, the combination of dissipative and purely reactive silencers defines the hybrid silencer concept. Fig. 11 shows a conceptual hybrid system that consists of two identical dissipative silencers and a reactive chamber in between. The reactive chamber can be approximated as a Helmholtz resonator with a neck and cavity. The small gap between two extended inlet and outlet ducts acts as the neck and the chamber as the cavity. The dimensions of two dissipative silencers are the same as those described at the beginning of Section 3 with outer chamber diameter now fixed at $d_2 = 164.4$ mm, and for the resonator, $L_2 = 100$ mm, $L_{ext1} = 65$ mm, and $L_{ext2} = 30$ mm.While the duct porosity of 8% will later be modified in this section, the filling density will be retained the same at 200 g/l for all configurations.

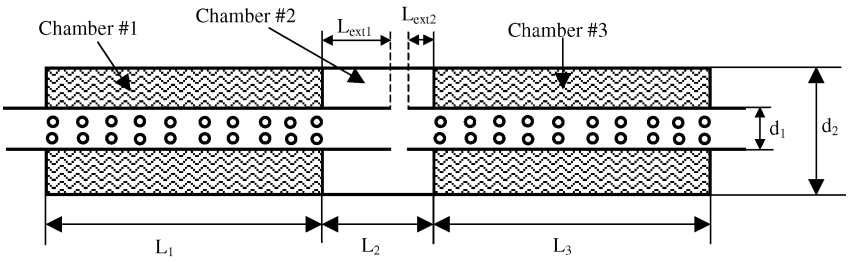

Fig. 11. A hybrid silencer: a Helmholtz resonator and two perforated absorbing silencers.

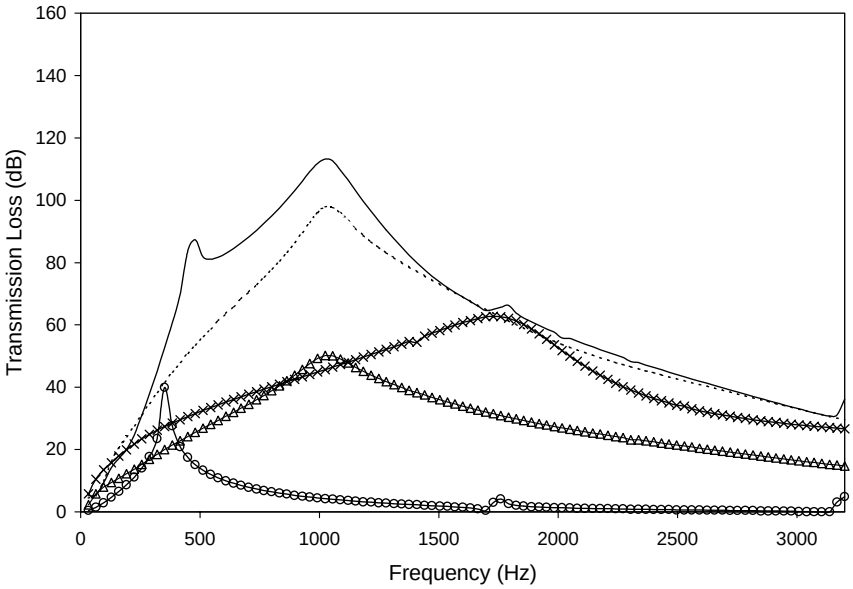

Fig. 12. BEM predictions for a hybrid silencer with $d_2 = 164.4$ mm and $\rho_f = 200$ g/l: —△—, chamber #1; —○—, chamber #2; - - - -, chamber #1,3; ——, chamber #1,2,3 (hybrid); — × —, chamber #4 (500 mm long).

Fig. 12 shows the BEM predictions for the hybrid silencer and its components, given in Fig. 11, with 8% duct porosity. The hybrid silencer (chambers #1, 2, 3 in Fig. 11) shows significantly higher transmission loss, for the overall frequency range, than the one with single chamber (#1). Connecting two dissipative chambers (#1 and #3) without a Helmholtz resonator (#2) nearly doubles the transmission loss of a single chamber (#1). Comparison of the two dissipative chambers (#1 and #3) with the hybrid silencer (chambers #1, 2, and 3) illustrates that a reactive element or Helmholtz resonator improves the noise reduction at low frequencies. For comparison purposes, the transmission loss of a 50 cm long single chamber dissipative silencer (designated by chamber #4) is also presented in Fig. 12. The geometrical details of chamber #4 are the same as described in Fig. 1 except for the total length. Note that compared to two dissipative chambers (#1 and #3) with the same total length (500 mm), the single dissipative chamber (#4) shows lower transmission loss for the overall frequency range, except at low frequencies, and peak transmission loss at higher frequencies.

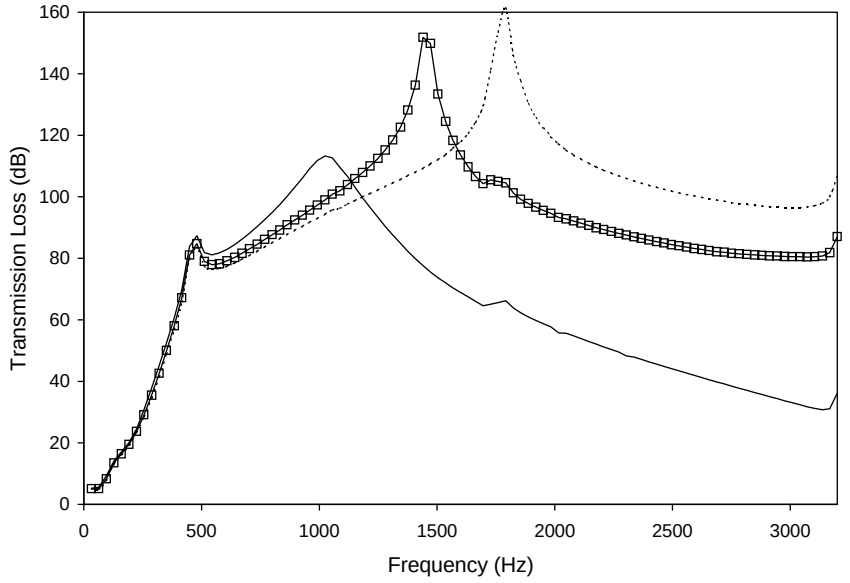

Fig. 13. BEM predictions for a hybrid silencer with $d_2 = 164.4$ mm and $\rho_f = 200$ g/l: ——, 8% porosity; —□—, 23% porosity; - - - -, 99% porosity.

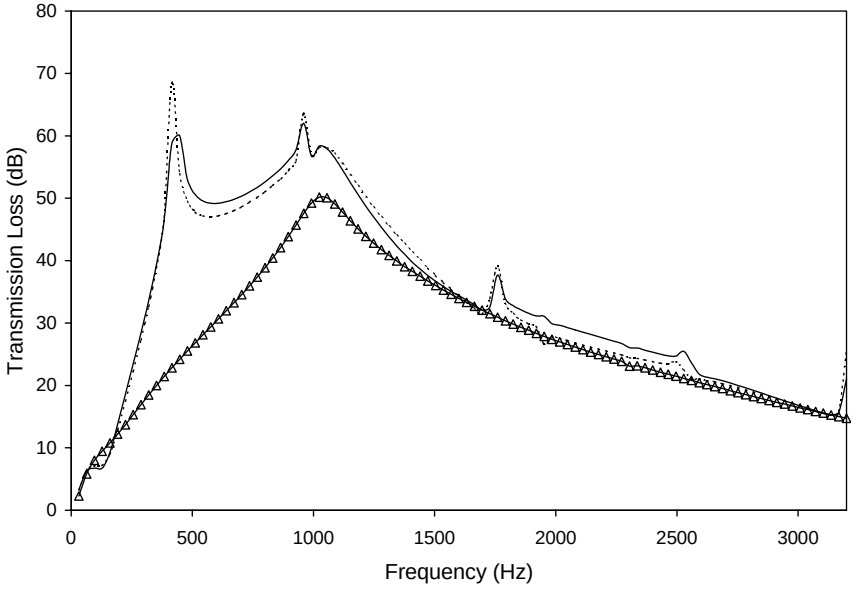

Fig. 14. BEM predictions for a hybrid silencer (chambers #1 and 2) with $d_2 = 164.4$ mm and $\rho_f = 200$ g/l: —△—, chamber #1 only; ——, chamber #2 followed by chamber #1; - - - -, chamber #1 followed by chamber #2.

The hybrid silencer (chambers #1, 2, and 3) in Fig. 12 has the transmission loss higher than 80 dB at mid-frequency range (450–1400 Hz); however, the transmission loss somewhat deteriorates at high frequencies. To improve the performance of hybrid silencers at high

frequencies, duct porosity is increased next from 8% to 23% and 99%, and the results are given in Fig. 13. Fig. 13 predicts that higher duct porosity can significantly improve the acoustic performance of a hybrid silencer at high frequencies. Unlike an unfilled perforated duct with 23% porosity acting like an expansion chamber (at the present length) due to negligible perforation impedance, high duct porosity for dissipative silencers can be considerable because the filling may increase the perforation impedance. Increasing the duct porosity does not influence the transmission loss below 500 Hz.

Fig. 14 shows BEM predictions for the hybrid silencer that consists of only chambers #1 and #2 in Fig. 11, and with 8% duct porosity. Placing reactive component (#2) ahead of the dissipative chamber (#1) slightly changes transmission loss. Fig. 14 also demonstrates that two-chamber hybrid silencers may have a slightly lower transmission loss at low frequencies (100–200 Hz) compared to the single dissipative chamber.

4. Conclusions

The acoustic performance of a single-pass perforated silencer has been investigated experimentally and analytically followed by a BEM study of a hybrid concept. The study has first considered single-chamber dissipative silencers with fixed 8% duct porosity and varying outer chamber diameter (101.0 and 164.4 mm) and filling material density (100 and 200 g/l). Increase in the filling density from 100 to 200 g/l has lowered the resonance frequencies and increased the magnitude of the transmission loss for both dissipative silencers with two different outer chamber diameters. Changing chamber diameter from 101.0 to 164.4 mm shifts the resonance frequencies lower for both material densities, but unlike the reactive chambers, may not increase the magnitude of peak transmission loss. Three-dimensional BEM shows good agreement with experimental results for the entire frequency range of interest.

The BEM is also used to predict the acoustic behavior of a hybrid silencer and its components. The reactive element or a Helmholtz resonator combined with two dissipative chambers can increase the transmission loss at low frequencies leading to effective hybrid silencers. The high duct porosity can improve the acoustic behavior of dissipative silencers at high frequencies. A silencer with two (250 mm long) chambers may have higher transmission loss and lower peak frequency than one with 500 mm long single chamber. The location of a reactive element may affect the overall acoustic behavior of a hybrid silencer.

The present study has thus (1) illustrated the effect of outer chamber diameter and filling material density on the acoustic attenuation of a single dissipative silencer; (2) improved the understanding of hybrid silencer behavior; and (3) demonstrated the benefit of BEM in predicting the transmission loss of dissipative and hybrid silencers. The study has assumed, however, a constant temperature inside the silencer in the absence of mean flow. Therefore, the impact of temperature and mean flow is yet to be explored. Furthermore, the effects of partial fiber fillings, location and distribution of perforations, and the shape of the reactive chamber remain to be investigated.

Acknowledgements

The first two authors would like to acknowledge (1) the support provided by Owens Corning Automotive for this work, and (2) many useful discussions with Dr. Richard D. Godfrey and Karl B. Washburn, and the assistance of Dr. Minor Nice who provided the data for Eqs. (22) and (23).

Appendix A. Empirical formulation of Delany and Bazley [7]

Delany and Bazley [7] presented empirical expressions for the complex-valued characteristic impedance and wave number of an absorbing material as follows:

$$\frac{\tilde{Z}_a}{Z_0} = [1 + 0.0511(f/R)^{-0.75}] + \mathrm{i}[-0.0768(f/R)^{-0.73}], \tag{A.1}$$

$$\frac{\tilde{k}}{k} = [1 + 0.0858(f/R)^{-0.70}] + \mathrm{i}[-0.1749(f/R)^{-0.59}], \tag{A.2}$$

where f (Hz) denotes frequency and R (mks Rayls/m) the resistivity.

Appendix B. Nomenclature

c_0	speed of sound in air (m/s)
$\tilde{c}$	complex speed of sound in the absorbing material (m/s)
d_1	perforated duct inner diameter (m)
d_2	outer chamber inner diameter (m)
d_h	perforate hole diameter (m)
f	frequency (1/s)
i	$\sqrt{-1}$, imaginary unit
k	wave number in air (1/m)
$\tilde{k}$	complex wave number in the absorbing material (1/m)
ℓ	single chamber silencer length (m)
L_1	length of the first dissipative chamber of a hybrid silencer (m)
L_2	length of the reactive chamber of a hybrid silencer (m)
L_3	length of the second dissipative chamber of a hybrid silencer (m)
L_{ext1}	extended inlet length of the reactive chamber of a hybrid silencer (m)
L_{ext2}	extended outlet length of the reactive chamber of a hybrid silencer (m)
p_1	acoustic pressure in the perforated duct (Pa)
p_2	acoustic pressure in the outer chamber (Pa)
R	flow resistivity of the absorbing material (mks Rayls/m)
T_{ij}	transfer matrix elements
t_w	wall thickness of the perforated duct (m)
TL	transmission loss (dB)
u_1	acoustic velocity in the perforated duct (m/s)

u_2 acoustic velocity in the outer chamber (m/s)
x co-ordinate axis
Z_0 $\rho_0 c_0$, characteristic impedance of air (kg/(m^2 s))
$\tilde{Z}_a$ complex-valued characteristic impedance of absorbing material (kg/(m^2 s))

Greek symbols
ϕ perforated duct porosity
ρ_f absorbing fiber material bulk density (kg/m^3)
ρ_0 air density (kg/m^3)
$\tilde{\rho}$ complex dynamic density in the absorbing material (kg/m^3)
$\tilde{\zeta}_p$ non-dimensionalized acoustic impedance of perforate

Subscripts
0 air
1 perforated duct
2 outer chamber
f absorbing fiber material
h perforate hole
p perforate
w perforated duct wall

Superscripts
i inlet
o outlet
p perforate

References

[1] C.G. Cofer, F. Bielert, T. Kullman, Durability, acoustic performance and process efficiencies of absorbent fibers for muffler filling, Proceedings of the 1999 SAE Noise and Vibration Conference SAE P-342, 43–49, 1999-01-1655, 1999.
[2] A. Craggs, A finite element method for modelling dissipative mufflers with a locally reactive lining, Journal of Sound and Vibration 54 (2) (1977) 285–296.
[3] K.S. Peat, K.L. Pathi, A finite element analysis of the convected acoustic wave motion in dissipative silencers, Journal of Sound and Vibration 184 (3) (1995) 529–545.
[4] C.N. Wang, Numerical decoupling analysis of a resonator with absorbent material, Applied Acoustics 58 (1999) 109–122.
[5] J.W. Sullivan, M.J. Crocker, Analysis of concentric-tube resonators having unpartitioned cavities, Journal of the Acoustical Society of America 64 (1) (1978) 207–215.
[6] R. Kirby, Simplified techniques for predicting the transmission loss of a circular dissipative silencer, Journal of Sound and Vibration 243 (3) (2001) 403–426.
[7] M.E. Delany, E.N. Bazley, Acoustical properties of fibrous absorbent materials, Applied Acoustics 3 (1970) 105–116.
[8] B.H. Song, J.S. Bolton, A transfer-matrix approach for estimating the characteristic impedance and wave numbers of limp and rigid porous materials, Journal of the Acoustical Society of America 107 (3) (2000) 1131–1152.

[9] U. Ingard, R.H. Bolt, Absorption characteristics of acoustic material with perforated facings, Journal of the Acoustical Society of America 23 (5) (1951) 533–540.
[10] R. Kirby, A. Cummings, The impedance of perforated plates subjected to grazing gas flow and backed by porous media, Journal of Sound and Vibration 217 (4) (1998) 619–636.
[11] A. Selamet, I.J. Lee, Z.L. Ji, N.T. Huff, Acoustic attenuation performance of perforated absorbing silencers, SAE Noise and Vibration Conference and Exposition, April 30–May 3, SAE Paper No. 2001-01-1435, Traverse City, MI, 2001.
[12] Z.L. Ji, Q. Ma, Z.H. Zhang, Application of the boundary element method to predicting acoustic performance of expansion chamber mufflers with mean flow, Journal of Sound and Vibration 173 (1) (1994) 57–71.
[13] C.-N. Wang, C.-Y. Liao, Boundary integral equation method for evaluating the performance of straight-through resonator with mean flow, Journal of Sound and Vibration 216 (2) (1998) 281–294.
[14] L.L. Beranek, Noise and Vibration Control, Institute of Noise Control Engineering, Washington DC, 1988.
[15] N.T. Huff, Materials for absorptive silencer systems, SAE Noise and Vibration Conference and Exposition, April 30–May 3, SAE Paper 2001-01-1458, Traverse City, MI, 2001.
[16] M. Nice, Owens Corning Automotive, Internal report, 1999.
[17] M. Nice, D. Godfrey, Measurement of characteristic impedance and propagation constant for trim packages, Proceedings of the First International AutoSEA Users Conference, July 27–28, San Diego, CA, 2000.
[18] A. Selamet, N.S. Dickey, J.M. Novak, Herschel-Quincke tube: a theoretical, computational, and experimental investigation, Journal of the Acoustical Society of America 96 (5) (1994) 3177–3185.